VNIR hypersensor camera system

David B. Cavanaugh, James M. Lorenz, Nora Unwin, Mark Dombrowski,

Surface Optics Corporation, San Diego, CA

Paul Willson

U.S. Army Armament Research and Development Engineering Center, Picatinny Arsenal

ABSTRACT

The hypersensor camera operates with a unique multispectral imaging modality developed recently at Surface Optics Corporation. The Hypersensor camera is small, low cost, rugged, and solid state, using micro-optics and an array of spectral filters, which captures a complete multispectral cube of spatial and spectral data with every focal plane exposure. The prototype VNIR Hypersensor camera captures full cubes of 588x438 (spatial pixels) x 16 (spectral bands) at frame rates up to 60 Hz. This paper discusses the optical design of the Hypersensor camera, the measured performance, and the design and operation of a custom video-rate hyperspectral processor developed for this system.

KEYWORDS

Hyperspectral, multispectral, video-rate, Bayer Filter, hyperspectral processor, spectral filter array, microlens array

1. INTRODUCTION

Multispectral and hyperspectral imaging systems (MSI, HSI) generate imagery that contains two-dimensional spatial imagery and one dimension of spectral information. Spectral imaging is thus inherently a three-dimensional process. Since focal plane arrays provide two-dimensional information, there are two predominate methods for integrating simultaneous spectral measurement with the spatial imaging process.

The first general method is to image the scene through a slit/spectrometer with multiple focal plane exposures, scanning the image piece wise over the detector. The scanning process can use either a scan mirror, or the motion of the sensor platform. Examples of multispectral systems are the LANDSAT and IKONOS imaging satellites, which combine the forward motion of the satellite with a cross-track scan mirror. Another common example is the family of hyperspectral imagers that use a moving scan mirror to capture a sequence of spectral “slices” from the scene. These systems generate highly detailed spectral imagery.

The second general method, which includes the system described in this work, subdivides the focal plane into an array of spectrally sensitive elements which capture the full spatial and

Imaging Spectrometry XIV, edited by Sylvia S. Shen, Paul E. Lewis, Proc. of SPIE Vol. 7457,
74570O · © 2009 SPIE · CCC code: 0277-786X/09/$18 · doi: 10.1117/12.833539

spectral qualities of the scene with each exposure of the focal plane. The most common example of this form of imaging is the Bayer filter [1], which separate the scene image on a focal plane into interleaved red, green and blue (RGB) spectral components. When these filter responses are matched to the human eye response realistic color images can be rendered from the encoded data.

The success of the Bayer filter approach arises from several factors. The RGB spectral filters each have a broad spectral bandpass that enables them to be fabricated from inexpensive spectral dyes. The filter elements can be precisely applied with photolithography. The groups of RGB filter elements are small and interleaved so that edge or point features in the image field do not create noticeable color anomalies in the imagery.

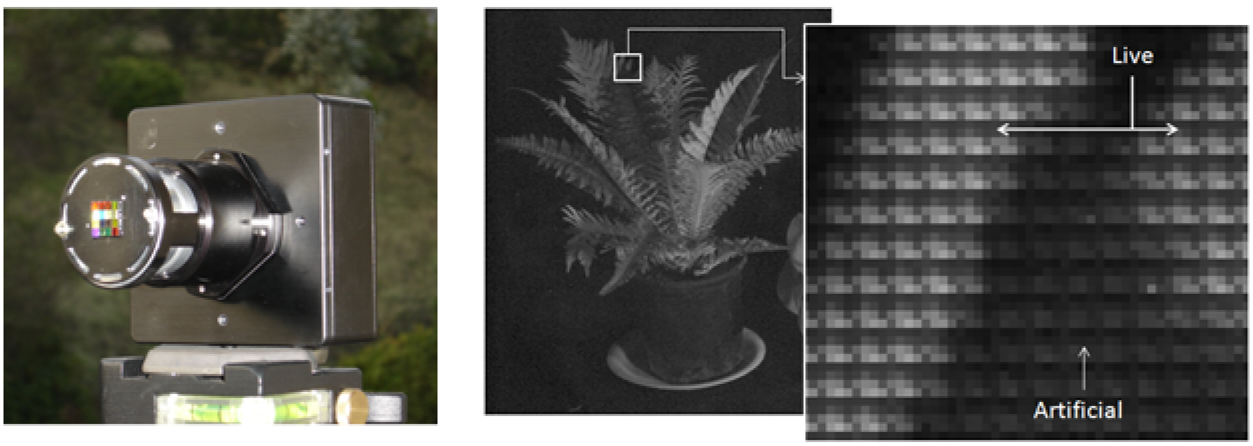

Figure 1: The prototype Hypersensor camera captures a sixteen-band multispectral 588 x 438 image with each focal plane exposure. The imagery produced by the Hypersensor consists of interleaved spectral superpixels. A live fern leaf shows chlorophyll activity in the magnified superpixel image, while an artificial fern leaf does not.

Extending the Bayer filter approach to a multispectral imaging system using a larger number of spectral filters than four becomes problematic. As the number of spectral filters increases the bandwidth of the filters must decrease, precluding the use of simple dyes. Dielectric stack filters are then required to achieve narrower and sharper pass bands. Such filters are difficult and expensive to fabricate and incorporate optically with the focal plane on a microscopic scale,

A multispectral imaging system that uses a set of filters that are large in size (compared to the size of a focal plane pixel) has several advantages over a multispectral Bayer approach. 1) the filters would be relatively inexpensive to fabricate, 2) the spectral bandpasses of the filters used can be of any type, i.e. narrow band, broadband, multi-band, etc. 3) The spectral bandpass of this filter set can be tailored to adapt the camera for the efficient detection of specific spectral signatures [2], and 4) the filter set can be changed easily.

This work describes an alternative multispectral modality to the Bayer filter method that allows the incorporation of a higher number of spectral bands. It uses a mosaic filter array (MFA) of spectrally selective filters as the spectral analysis elements. The MFA is macroscopic in size, and is placed at the pupil of the objective lens. A micro-lens array (MLA) is incorporated as an imaging element that simultaneously combines the spectral and the spatial imaging dimensions.

2. SYSTEM DESCRIPTION

The Hypersensor prototype camera is shown in Figure 1. This camera is based around the Dalsa 4M60 Pantera body and focal plane. The objective lens is an SOC custom telecentric design. A Mosaic Filter Array (MFA) of sixteen narrowband spectral filters is

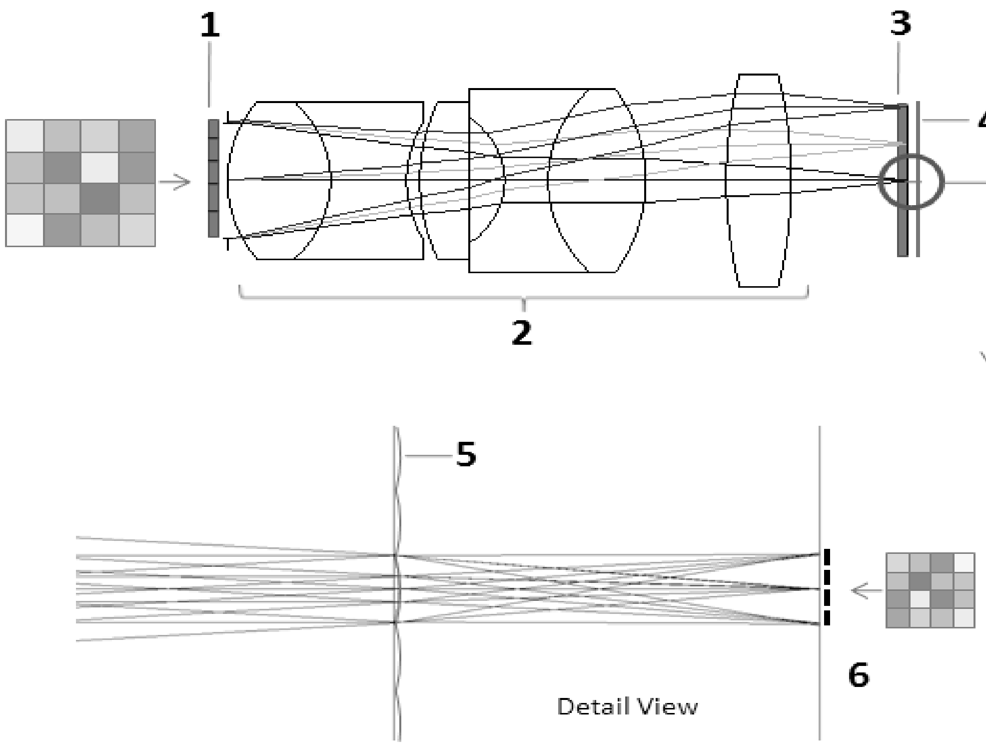

Figure 2: The Hypersensor layout is shown in the upper diagram. The MFA (1) is placed at the stop of the telecentric objective lens (2). The MLA (3) is located in close vicinity of the focal plane. A detailed view of the focal plane region (lower figure) shows the objective lens image formed just behind the MLA lenslet plane (5). Each lenslet forms a conjugate real image of the MFA on the focal plane (6). The focal plane array is aligned with these replicated images so that each FPA pixel recieves light from only one filter of the MFA. The MFA images are replicated over the entire focal plane.

mounted at the stop of the objective lens. A microlens array (MLA) is mounted internally in close proximity to the focal plane array, and requires no additional volume or added mass. The entire camera is no larger than a standard panchromatic camera. The camera is fully solid state with no moving parts.

The optical system design is comprised of four main components, illustrated in Figure 2. The MFA (1) consists of a set of spectrally selective filters, and is mounted at the stop of the image-telecentric objective lens. The objective lens (2) produces a real image of the scene captured through the MFA in the plane of the MLA (3, 5). Each lenslet of the MLA (5) forms a unique conjugate image of the objective's pupil (i.e. MFA), on the focal plane array: (4, 6). Figure 2 shows a single MFA image, but in reality each lenslet forms a unique image, and these images sit edge-to-edge covering the entire focal plane.

The magnification of the conjugate lenslet images on the focal plane is determined by the lenslet power. The magnification is set such that the lenslet image of the NxN MFA exactly matches the size of an NxN group of pixels (i.e. superpixel) on the focal plane. The lenslet images are replicated across the focal plane, with the images touching edge-to-edge. Thus, when the MLA is aligned with the focal plane array each pixel in the superpixel group receives light from a single filter in the mosaic array.

The hypersensor can be designed with different numbers of spectral filters in the MFA. The prototype system uses a 4x4 MFA, which provides 16 spectral samples. A 3x3 or 5x5 MFA could also be used. Decreasing the number of filters increases the spatial resolution of the images. Experiments have shown that 16 multispectral bands is sufficient to detect specific gaseous chemicals with nearly the same reliability as can be obtained from hyperspectral images with hundreds of bands.[]

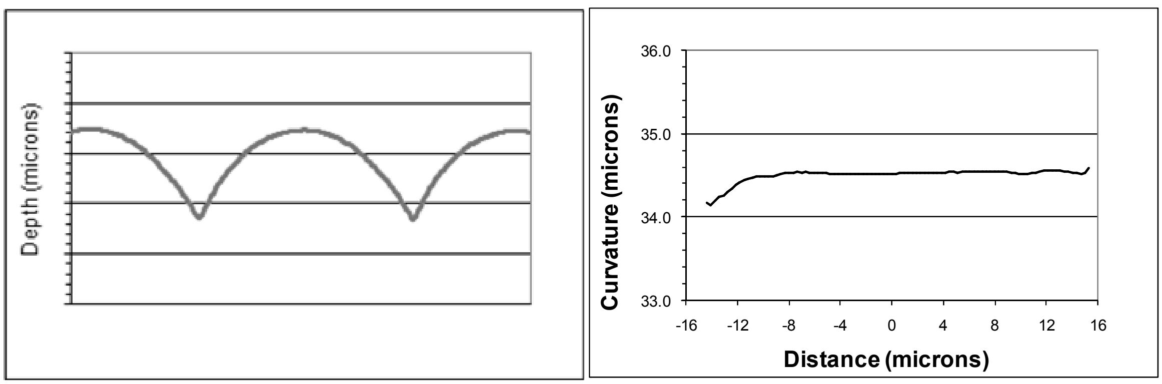

Figure 3: The microscopic optical quality of the MLA used in the prototype system was measured at SOC with an atomic force microscope, (upper left). The plot on the right is the radius measured from the center of curvature to the measured points. The flat line indicates the lenslet surface is spherical.

Micro Lens Array:

The MLA lenslets form images over a broad spectral range, and thus a spherical surface figure for these lenses is optimal. The profile of the MLA in the prototype system was measured with an atomic force microscope. Figure 3 shows a profile drawn across the vertex of a lenslet. Also shown is a plot of the radius taken from the center of curvature to the series of measured points on the lenslet surface. A spherical lens should show uniform radius across the lenslet. The measurement shows the lenslets are spherical over the most of the lenslet area, with some minor deviations.

Objective Lens:

The objective lens has several requirements. The objective lens must be chromatically balanced over the entire spectral range. The stop of this lens is ideally located where the cone of rays is smallest, to optimize the bandpass filter performance. The lens must be image-telecentric. This ensures that each MLA lenslet, the conjugate image, and the superpixel region of the focal plane are each coaxial with the chief ray, at all points in the image field.

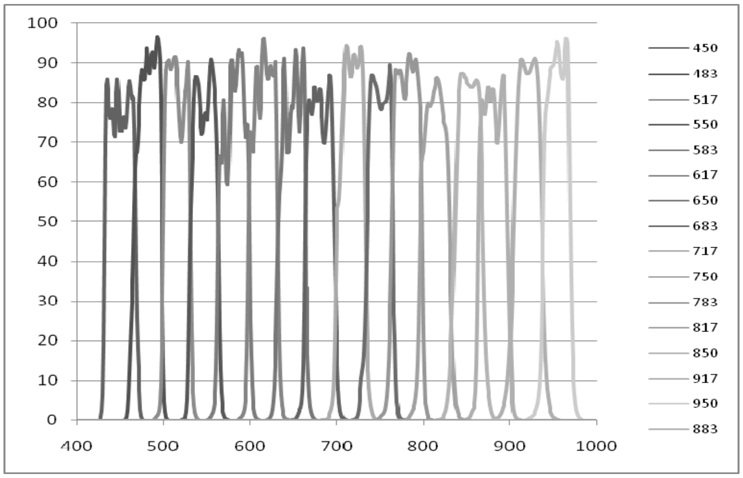

650	820	780	750
550	480	450	520
620	910	950	580
720	850	880	680

Figure 4: The spectral bandpass of the prototype filters is shown. The table gives the layout of the wavelengths in the MFA and superpixel. The values shown are the center wavelengths in nanometers.

Mosaic Filter Array

The MFA is an array of spectrally selective filters. The MFA filters can have any spectral bandpass that is within the spectral response of the focal plane array. Figure 4 shows the evenly spaced bandpass distribution of the MFA employed in the prototype system. This MFA was made by fabricating each filter type on large wafers, dicing the finished wafers to size, then edge-bonding these parts into the mosaic structure. Care must be taken to ensure the assembled filter elements are optically coplanar. The filter array could also be produced on a single substrate with photolithography, ensuring co-planarity of all elements, but at a higher fabrication cost.

Focal Plane Array

The focal plane array must have a high pixel count to achieve high spatial and spectral resolutions. For example, in order to produce an image with 588x438 spatial resolution with 16 spectral bands per pixel we would require a focal plane with a
2352x1756 pixel count. The MLA must be brought into close proximity with the focal plane array, aligned precisely with it, and then bonded in place. The focal plane
mechanical layout must provide access for the MLA to be brought close to the focal plane surface. Larger focal plane pixels are beneficial in order to minimize diffraction by the MLA lenslets, as discussed below.

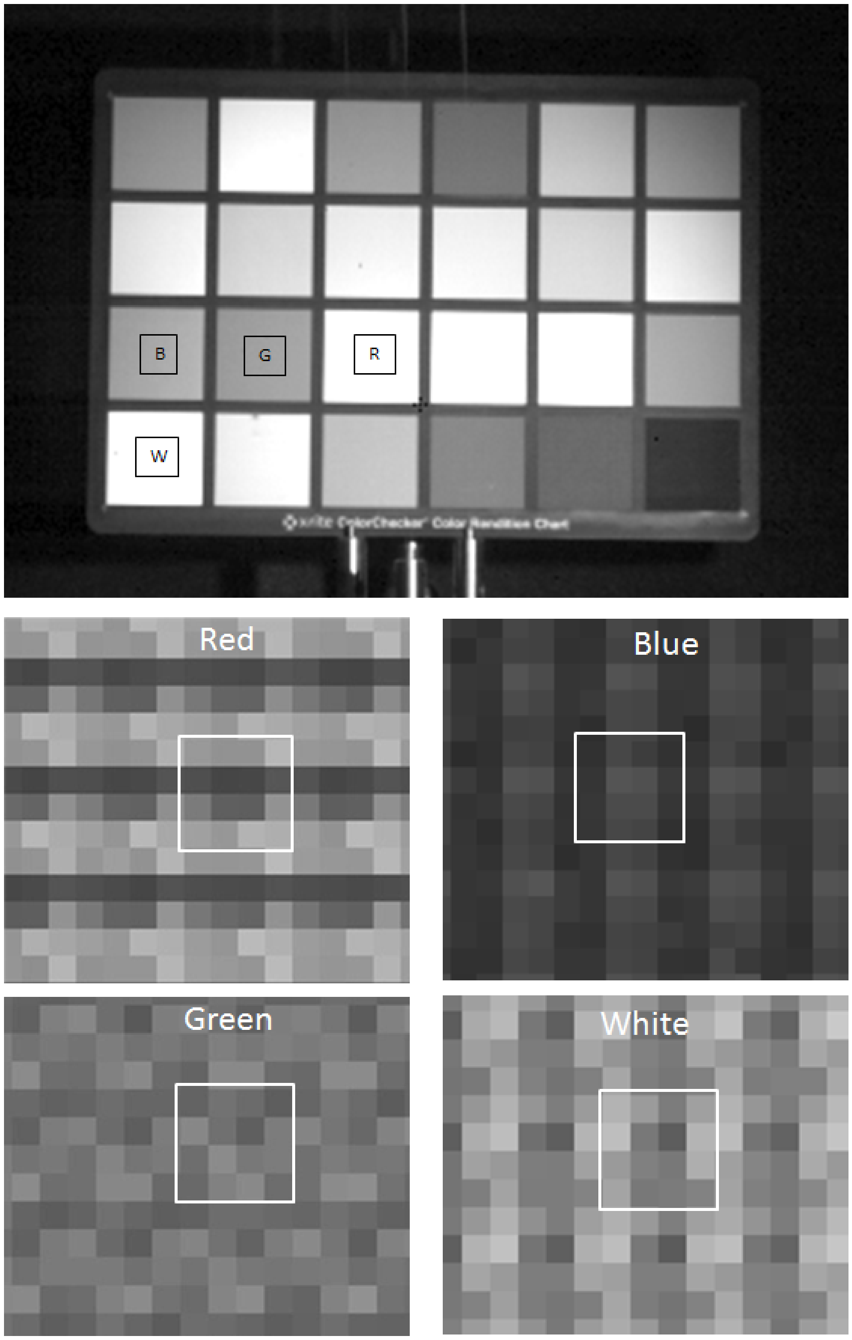

Figure 5: The top image is the 550 nm Hypersensor image taken of a Macbeth color chart. The four lower images are magnified views of the red, green, blue and white color squares, extracted from the raw Hypersensor image. The white boxes outline one 4x4 superpixel region. The variation in pixel intensity due to the color differences is evident.

MLA Alignment

The axes and plane of the MLA must be precisely aligned with the focal plane array through six degrees of freedom: spatial (x, y), focus (z), azimuth, roll and pitch. The MLA and FPA rows or columns are made parallel, the MLA plane is made exactly parallel to the FPA, and the lenslets are aligned in (x,y) to exactly overlay the superpixel groups. The MLA is focused with the FPA. These operations are all performed while observing live imagery through the foreoptic and MFA pupil. Once the alignment is achieved, the MLA is permanently bonded to the focal plane. The optical system is very stable once the MLA is aligned and set. No loss of alignment of the micro-optic and focal plane has been observed on the prototype systems after several months of operation and handling.

3. SPECTRAL IMAGING

The imagery produced by the hypersensor is of high quality. Figure 5 is the 650 nm Hypersensor image taken of a Macbeth color chart. This image was extracted from the raw image by taking the specific 650 nm pixel from each superpixel. The dimensions of each extracted image are 588x438 pixels. There are 16 such spectral images obtained from each raw image captured from the camera.

Four of the color regions (red, green blue and white) from the raw image are shown highly magnified, illustrating the superpixel detail in Figure 5. The wavelength map for the superpixels was given in Figure 4.

The spectra extracted from the superpixels shown in Figure 5 are plotted in Figure 6. The Hypersensor reflectance spectra were normalized using the white box on the color chart. Also plotted are the absolute reflectance spectra measured from the same areas with a Cary spectrophotometer. The spectral shape and general magnitude of the Hypersensor measurements are seen to correspond well with the absolute measurements.

It must be noted that constant offsets were subtracted from the Hypersensor spectral curves shown in Figure 6 to match the Cary curves. The magnitude of these offsets varied with the spectral content of the scene, and ranged around 50 to 100 digital values. The Hypersensor data contains offsets due to diffraction effects in the microlens array, where energy from one spectral component leaks into its neighbors. This is discussed in the next section.

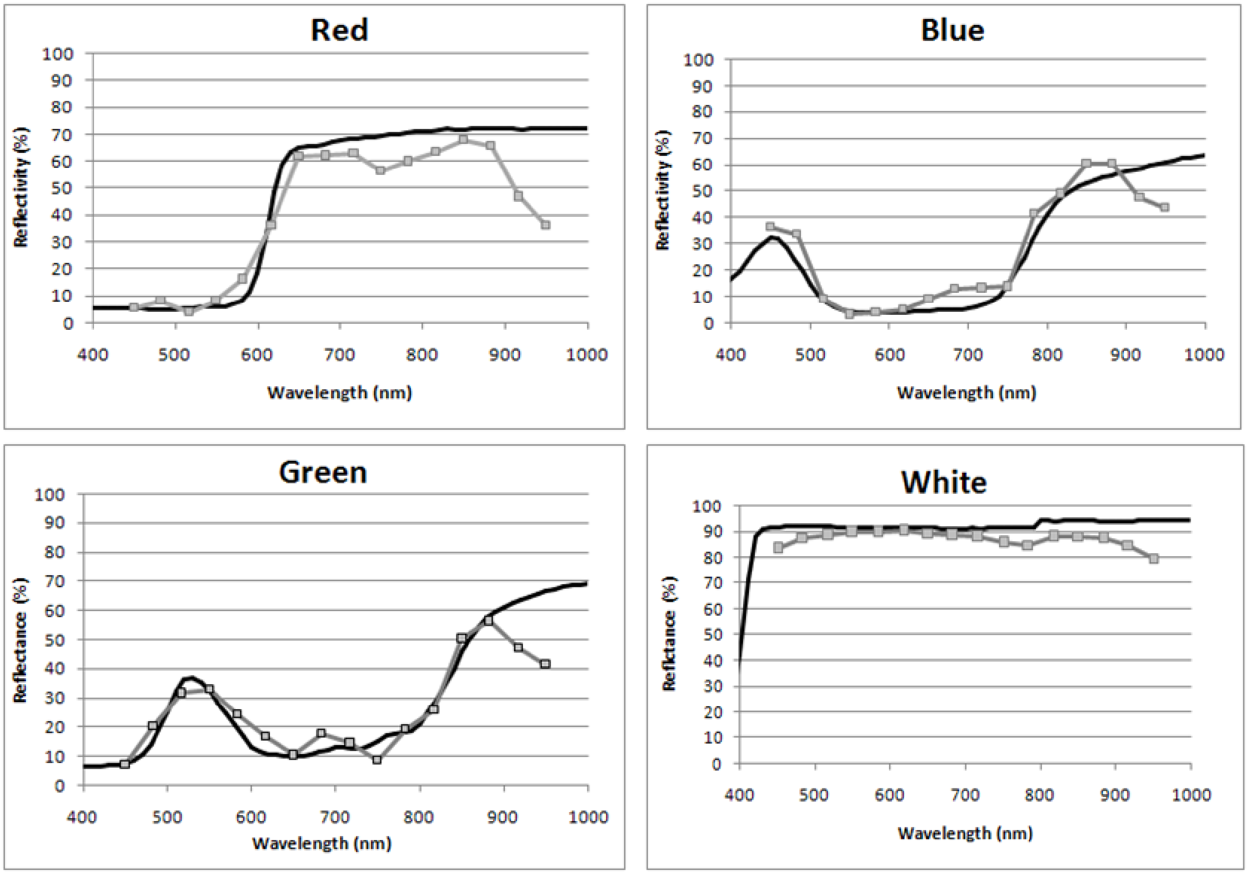

Figure 6: The Red, green, blue and white spectra measured from the superpixels shown in Figure 5 are plotted in gray. The % reflectance curves for the same areas are plotted in black. Small offset corrections were applied to the Hypersensor spectra to achieve overlap.

4. LENSLET DIFFRACTION

When the Hypersensor images a monochromatic field of light a single filter of the MFA will ideally irradiate only a single pixel within each superpixel group. This pixel would then receive all of the energy, and the surrounding pixels would be dark. However, the MLA lenslets are essentially an array of apertures which have a size that is approaching the wavelength of light, and diffraction from these apertures causes light to spread into the adjacent pixels.

Figures 8 shows a magnified 12x12 pixel region of the focal plane for illumination by two uniform monochromatic sources. A significant fraction of the energy is diffracted into the neighboring pixels, particularly at longer wavelengths.

The leakage is seen in the imagery as an increase in the image background, similar to a dark current. The level of the leakage background is dependent on wavelength, since the diffraction effects are more pronounced at longer wavelength. Thus, regions of the imagery weighted toward longer wavelength will show a higher leakage background than imagery which contains predominantly shorter wavelength. Methods for mitigating diffraction effects are currently in development at SOC.

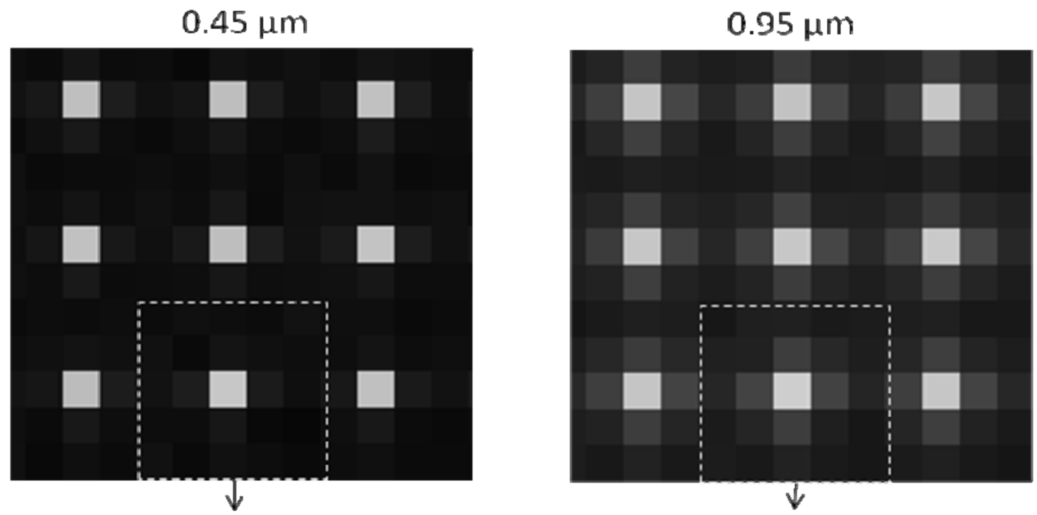

0	0.017	0.034	0.017	0
0.017	0.025	0.091	0.025	0.017
0.034	0.100	**1.0**	0.100	0.034
0.017	0.025	0.093	0.025	0.017
0	0.017	0.034	0.017	0

0	0.078	0.120	0.078	0
0.078	0.130	0.266	0.130	0.078
0.120	0.32	**1.0**	0.32	0.120
0.078	0.130	0.276	0.130	0.078
0	0.078	0.120	0.078	0

Figure 8: A uniform field of monochromatic light at two wavelengths, imaged by the Hypersensor. Diffraction at the lenslets causes leakage into the neighboring pixels. The relative leakage, mapped in the tables, is seen to be a strong function of wavelength.

5. POINT SOURCES

The Hypersensor scene in Figure 7 contains a tiny ball bearing on a black background which produces a small bright glint (pointed to by the arrow). The raw superpixel image of this point contains both the spectral and spatial information. Each of the single-wavelength images shows this point source as a small cluster of bright pixels.

This is a significant result. There are prior systems [4] that use micro-optical elements on the focal plane for spectral or polarimetric analysis. These systems do not use microlenses to delineate the IFOV as a cluster . Each individual spectral or polarimetric resolution elements is then the IFOV. There are thus spatial displacements between the spectral samples.

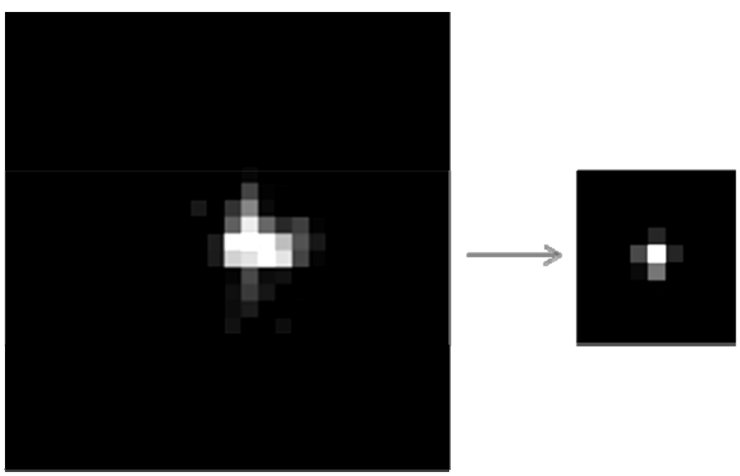

Figure 7: The Hypersensor image contains a small point source (see arrow). The raw image of the glint taken with the Hypersensor is shown below to the left. When single wavelength images are extracted (below, right) a single bright point is observed at each wavelength.

Any contrast in the imagery (i.e. points or lines) thus produces anomalous distortions of the spectral or polarimetric measurements.

The Hypersensor design solves this problem with microlenses. Each microlens forms an image of the pupil where the spatial scene information is homogenous. Thus, under standard operating conditions edge or point contrast variations contained in the IFOV regions do not distort the spectral measurements when imaged at the focal plane.

6. VIDEO RATE PROCESSING

The Hypersensor camera is designed to operate as a video-rate multispectral imager. A method for extracting useful information from the data at video rates is thus a necessary component of the system. A real time video processor system was designed for the Hypersensor camera, which consists of a PC-104 computer running Windows XP and two custom interface/processor cards: the Camera Interface, and the MIDIS Processor Boards. The prototype video processor is shown in Figure 8.

Figure 8: The Hypersensor camera installed with the hyperspectral video processor system is a compact data collection system that requires only a display, keyboard and mouse to operate.

Camera Interface Board

The Camera Interface Board, shown schematically in Figure 9, receives the image data and framing signals from the camera. It independently controls two CameraLink cameras, though only one interface is used for the present Hypersensor system. It provides four signal lines to the camera, only one of which is currently used. This control line provides variable pulse widths, where the pulse rate determines the frame rate of the camera, and the pulse width determines the integration time. The Camera Control interface controls the camera functions over the serial interface in the Camera Link, and receives status messages from the camera.

The Computer Interface block receives data from the embedded computer. It allows the computer to set various registers within the chip to control the operation of the interface, as well as provide a fast upload/download capability that allows the embedded computer to load or read any of the memory locations on the board.

The Memory Remapper and Storage Block take the four input data streams and writes them out to one of the external SSRAMs. Each of the SSRAMs is capable of storing one entire frame of data. Once a frame is completely received it is output to the Multi-Cube Storage Block. While this is being output another frame of data can be stored in a second external SSRAM. The two memories can be used in ping-pong fashion for storage and readout to maintain the maximum frame rate of the camera. A third SSRAM can be used that provides the mapping of the incoming data into the external memories so that when it is read out it will be in the correct processing format. All three SSRAMs can download/upload to the embedded computer.

The Multiple Cube Storage block provides the capacity for capturing 64 full frames of data, and is stored in external DDR-2 SDRAM.

Processor Board

The Processor Board, shown in Figure 10, receives BIP formatted data from the Camera Interface board as four 16-bit data words running at half the processing rate. These are multiplexed in the Input Interface Block into two 130 Mpixel/sec data streams and sent to the Image Calibration block.

The Calibration block performs a simple two step calibration on the incoming data. It first subtracts a stored dark level, and then performs a gain correction to the data. The dark level subtractions are stored as 16 bit fixed-point data. The gain calibration coefficients are 18 bits in length, with14 bits of mantissa and a four bit exponent. The output of the gain correction is 16 bit fixed data.

The gain and offset calibration is followed by an optional radiance correction that compensates for the scene dependent light levels, so that the image data represents the pixel reflectance. Correction for atmospheric absorption can also be applied. The output is 24-bit fixed point data.

The Image Detection and Integration Block have eight matched filter blocks and two integrator paths that operate at 130MHz. The integrator blocks are triple integrators that output three 16-bit integers. The matched filters output 32-bit integer values. They can be independently configured to process Spectral Angle (SAM) filters, or to normalize the target and pixel vectors (ZMDA). The SAM algorithm is the basic dot product of the target: and pixel: vectors.

$$c_{SAM} = \frac{\mathbf{T} \bullet \mathbf{S}}{|\mathbf{T}||\mathbf{S}|} \qquad (1)$$

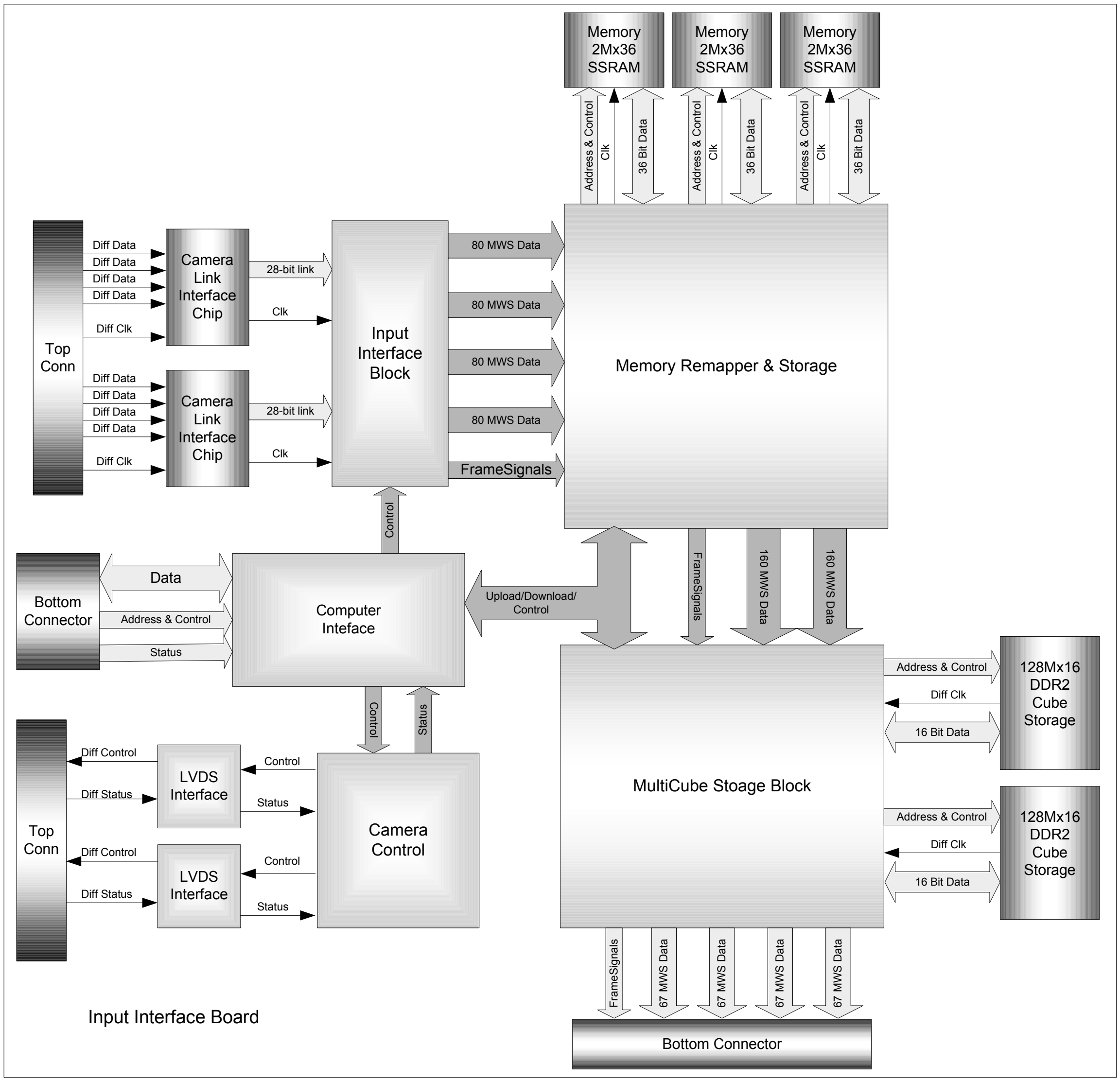

Figure 9: Block diagram of the Camera Interface board

The zero mean differential area (ZMDA) algorithm normalizes the target and pixel vectors by their variance and computes their difference, which corresponds to the area between the two vectors:

$$c_{ZMDA} = 1 - \sqrt{\sum_{N}\left[\frac{\mathbf{T}(\lambda_{\mathrm{n}}) - \langle \mathbf{T}(\lambda_{n})\rangle}{\sqrt{\sum\left(\mathbf{T}(\lambda_{\mathrm{n}}) - \langle \mathbf{T}(\lambda_{n})\rangle\right)^{2}}} - \frac{\mathbf{S}(\lambda_{\mathrm{n}}) - \langle \mathbf{S}(\lambda_{n})\rangle}{\sqrt{\sum\left(\mathbf{S}(\lambda_{\mathrm{n}}) - \langle \mathbf{S}(\lambda_{n})\rangle\right)^{2}}}\right]^{2}} \quad (2)$$

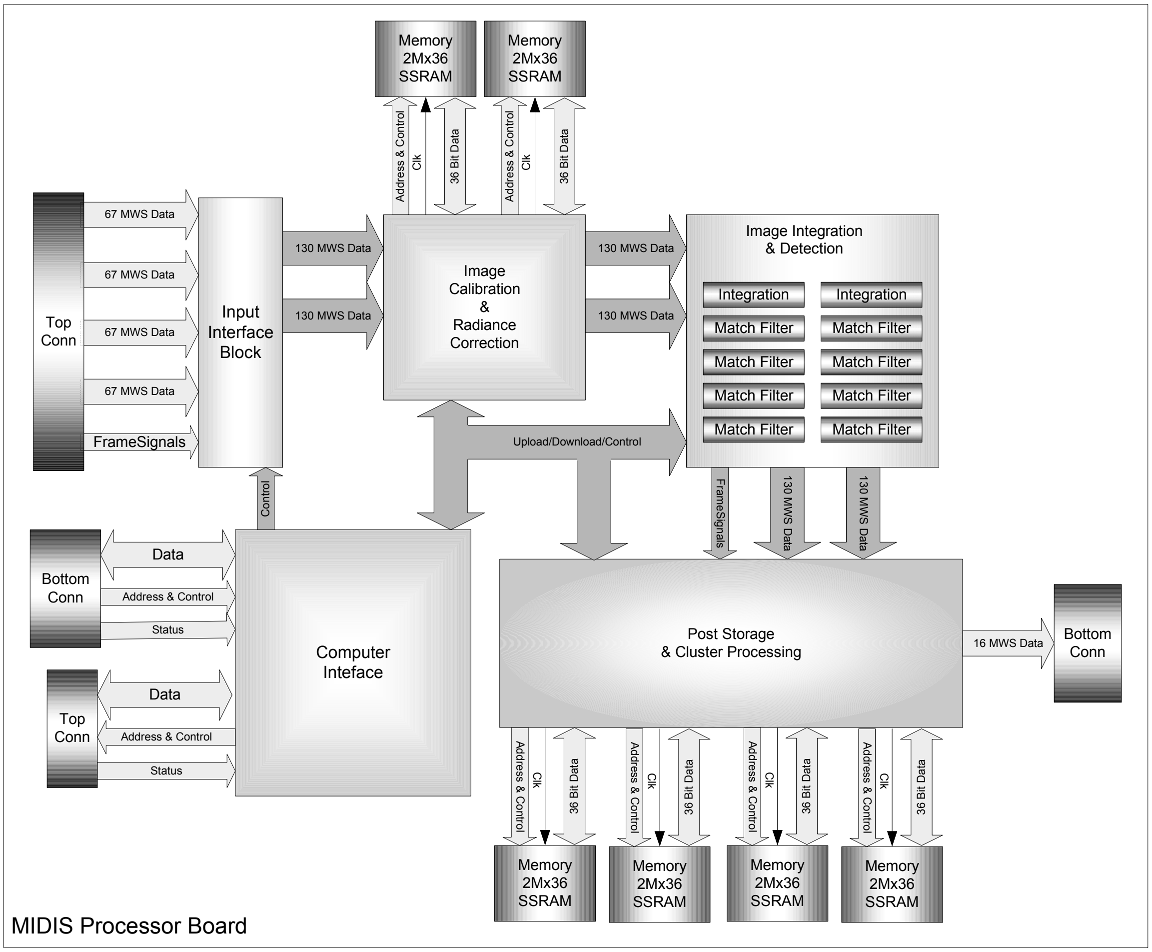

Figure 10: Block diagram of the MIDIS hyperspectral processor board

Other SAM variations are also currently programmed in the processors. Additional channels may be added if other matched filters, such as the Spectral Ratio [3] are desired.

The processed results are stored in the Post Storage and Clustering Block. This block takes the results from the previous block and stores them in external SSRAM.

The data that is sent to the embedded computer for display or storage is user-selectable. The output display can be the integrator, with the option to highlight areas that where the matched filter results are above a selectable threshold. The individual results of the matched filters will also be available for display. To help find the object in the scene that has the most matched filter results that are above threshold, the results of the matched filter are passed through a clustering algorithm. The result of this cluster processing will be to highlight only the area of the picture that has the largest contiguous pixels that are above threshold.

7. PROCESSING RESULTS

Figures 11 through 13 illustrate a Hypersensor image of a houseplant taken with the video processor system, in which a fraction of the leaves are artificial. Two ZMDA matched filters are enabled, and loaded with representative spectra (Figure 11) taken from the images of live and artificial leaves. The unfiltered image of the plant is shown at the top, which was formatted for this paper by converting the RGB image from the processor to grayscale.

When the "live leaf" channel detector is enabled, and the detection threshold is optimized, the living leaves are highlighted on the video display with a color overlay (which for channel 1 is typically red). The left image in Figure 13 shows this channel image, where all of the red detected pixels are set to white.

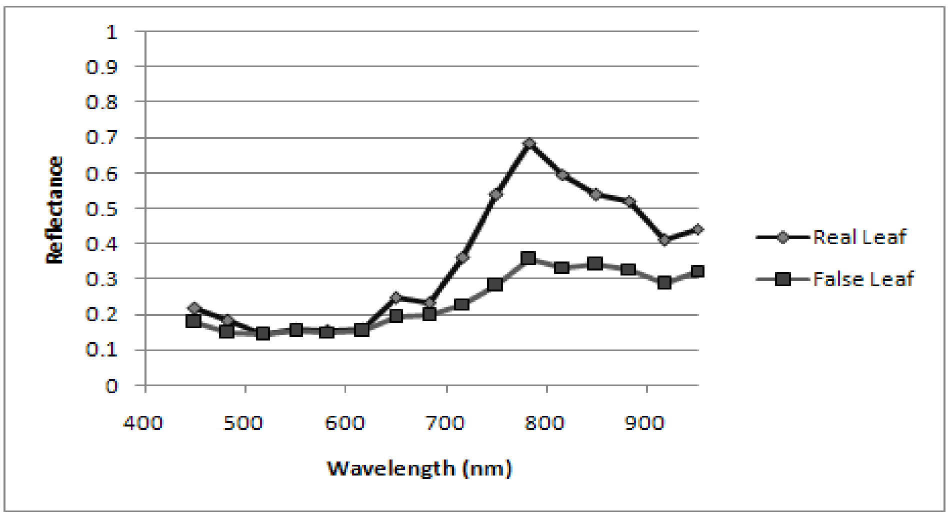

Figure 11: Spectral samples used in the processor example of Figure 12

Similarly, when the "artificial leaf" channel is enabled the false leaves are highlighted on the video display with a blue color for channel 2. The right image in Figure 13 shows the artificial leaves where the blue detected pixels are set to white.

The processor is currently configured for eight matched filter channels to be programmed and operated simultaneously. The two detection channels here were illustrated separately because the constraints for black and white printing. In reality these all detection channels run concurrently. It is also important to note that the results shown in Figure 11 are a video snapshot. The processor computes and displays these results at up to a 60 Hz frame rate.

8. APPLICATIONS

The Hypersensor imager was developed primarily as an application-specific multispectral imager. Unlike scanned hyperspectral imagers, the Hypersensor produces full image cubes at video frame rates, is low in cost, is intrinsically rugged, and can be miniaturized to a high degree. The hypersensor operates in a manner that is similar to standard panchromatic cameras, thus the installation and operation of the cameras is straightforward.

The hypersensor is useful for applications such as:

- High speed industrial inspection
- Aerial surveying from small UAV platforms
- High speed multispectral target detection
- Gas leak detection systems

The Hypersensor is adapted to a specific application by first establishing the number of wavebands, their center wavelengths and bandpasses from hyperspectral measurements. This optimal set of filters would then be fabricated into an MFA and installed in the camera. The vacuum deposition group at SOC is currently devising production strategies for minimizing the cost of manufacturing these filter arrays.

Figure 12: This plant contains a mixture or real and artificial leaves. The image was captured in RGB format from the hypersensor processor and converted to grayscale.

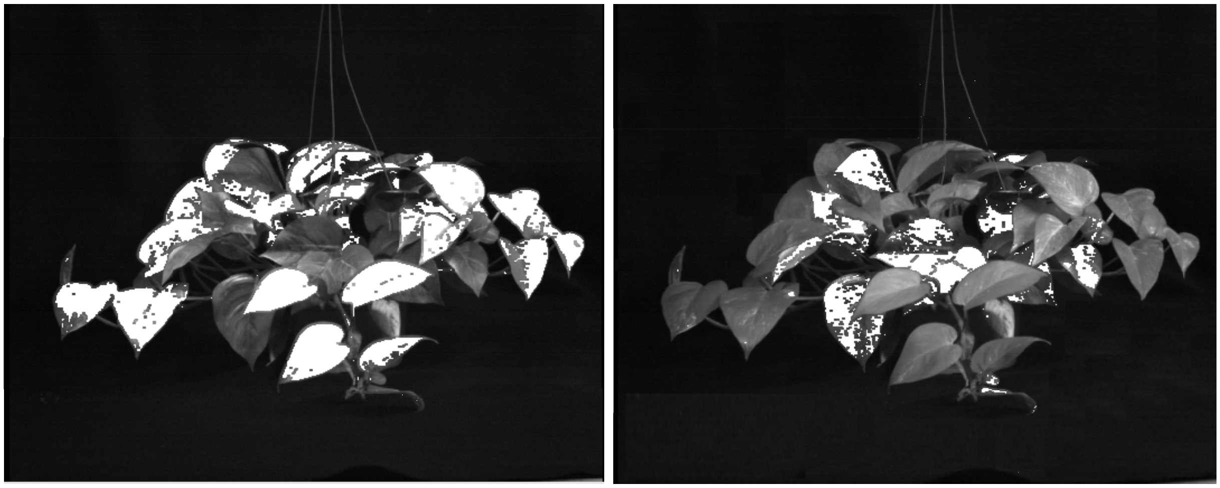

Figure 13: The hyperspectral video processor was set to detect the real leaves (left) and the artificial leaves (right) with the ZMDA algorithm. The detections are set to white for each case.

9. CONCLUSIONS

The hypersensor camera is a multispectral imager that provides high-spatial resolution multispectral cubes at video frame rates. The basic performance of the camera is proven and validated. The mitigation of diffraction effects in the imagery is currently in work at SOC.

10. REFERENCES

[1] Bayer, B.E., “Color Imaging Array,” U.S. Patent Number 3,971,065

[2] “Sparse linear filters for the detection and classification in hyperspectral imagery”; Theiler, J. and Glocer, K.; Proc. SPIE 6233 (2006)

[3] “Spectral Ratio of Reflectance for Estimating Chlorophyll Content of Leaf”; Inada, K.; Japan Jour. Crop Sci. 54(3): 261—265 (1985)

[4] Goldstein, D.H. and Chipman, R.A; “Infrared Spectropolarimeter”; U.S. Patent Number 3,971,065; Sept. 1991